

High efficiency n-type silicon solar cells featuring passivated contact to laser doped regions

Xinbo Yang, James Bullock, Qunyu Bi, and Klaus Weber

Citation: [Applied Physics Letters](#) **106**, 113901 (2015); doi: 10.1063/1.4915326

View online: <http://dx.doi.org/10.1063/1.4915326>

View Table of Contents: <http://scitation.aip.org/content/aip/journal/apl/106/11?ver=pdfcov>

Published by the [AIP Publishing](#)

Articles you may be interested in

[Passivating boron silicate glasses for co-diffused high-efficiency n-type silicon solar cell application](#)

Appl. Phys. Lett. **107**, 042102 (2015); 10.1063/1.4927667

[Amorphous silicon passivated contacts for diffused junction silicon solar cells](#)

J. Appl. Phys. **115**, 163703 (2014); 10.1063/1.4872262

[Aluminum-oxide-based inversion layer solar cells on n-type crystalline silicon: Fundamental properties and efficiency potential](#)

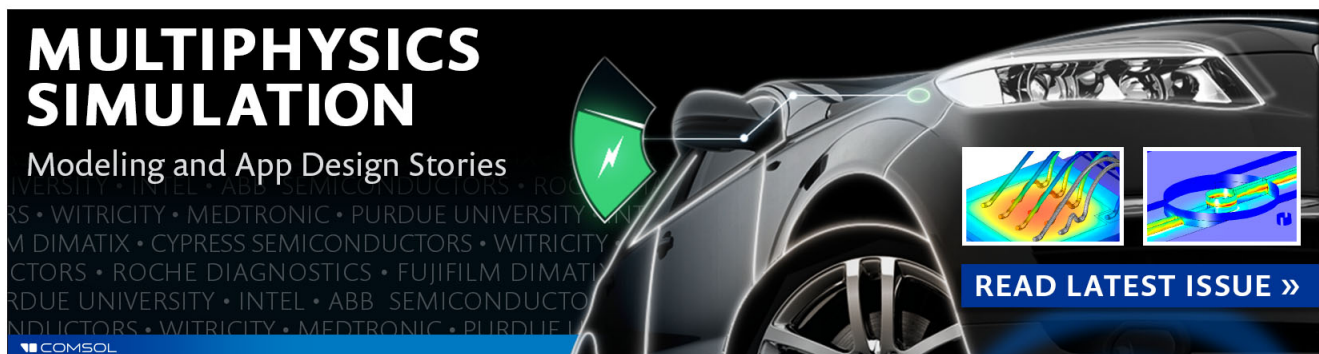
J. Appl. Phys. **115**, 073702 (2014); 10.1063/1.4865962

[Chemical etching of boron-rich layer and its impact on high efficiency n-type silicon solar cells](#)

Appl. Phys. Lett. **101**, 073902 (2012); 10.1063/1.4746424

[Capacitance study of inversion at the amorphous-crystalline interface of n-type silicon heterojunction solar cells](#)

J. Appl. Phys. **110**, 114502 (2011); 10.1063/1.3663433

The advertisement features a dark background with a car's front end on the right. On the left, the text 'MULTIPHYSICS SIMULATION' is written in large, bold, white letters. Below it, 'Modeling and App Design Stories' is written in a smaller white font. A green lightning bolt icon is positioned between the text and the car. On the right side of the car, there are two small inset images showing simulation results: one with a color gradient and another with a blue and yellow pattern. At the bottom right, a blue button with white text says 'READ LATEST ISSUE >>'. The COMSOL logo is visible in the bottom left corner.

**MULTIPHYSICS
SIMULATION**
Modeling and App Design Stories

READ LATEST ISSUE >>

COMSOL

High efficiency n-type silicon solar cells featuring passivated contact to laser doped regions

Xinbo Yang,^{a)} James Bullock, Qunyu Bi, and Klaus Weber

Research School of Engineering, The Australian National University, Canberra, ACT 2601, Australia

(Received 30 January 2015; accepted 8 March 2015; published online 16 March 2015)

Minimizing carrier recombination at cell contacts becomes increasingly important for reaching high efficiency. In this work, the passivated contact concept is implemented into n-type silicon solar cells with laser-processed local back surface fields. The passivation and contact characteristics of the SiO₂/amorphous silicon (a-Si:H) stack on localized laser doped n⁺ regions are investigated. We find that the SiO₂/a-Si:H stack provides not only good passivation to laser doped n⁺ regions but also allows a low contact resistivity after thermal annealing. With the implementation of the SiO₂/a-Si:H passivated contact, an absolute efficiency gain of up to 1.5% is achieved for n-type solar cells. © 2015 AIP Publishing LLC. [<http://dx.doi.org/10.1063/1.4915326>]

The main challenge in today's photovoltaics industry is to increase the conversion efficiency and to lower the production costs of cells. A route towards higher efficiency is via the implementation of selective emitter (SE) and local back surface field (LBSF) structures into silicon solar cells. A SE can reduce contact resistance by allowing heavy doping under the metal contacts, while ensuring low recombination elsewhere via lighter doping in the optically active regions, which results in a higher fill factor (*FF*) and a better blue response (higher short circuit density *J*_{sc}). A heavily doped LBSF can also increase the fill factor due to a decreased series resistance and rear-side recombination. The ultra-high efficiency passivated-emitter rear locally diffused (PERL) silicon solar cells have been fabricated with locally doped regions at front and rear sides.¹ However, the approach used to realize local doping requires cost-intensive and time-consuming processes, such as photolithography-based wet chemical processing and high temperature diffusions, which limit the commercial success of the PERL cell concept.

In recent years, laser processing has attracted considerable attention from industry as a fast and cost-effective technique for forming locally doped regions in silicon solar cells. High efficiency silicon solar cells with laser-doped SEs and/or LBSFs have been reported.²⁻⁵ An absolute efficiency gain up to 1% has been achieved with the implementation of laser-processed SE or LBSF. Recently, n-type PERL solar cells with an efficiency of up to 23.2% have been achieved using a laser-based *PassDop* technology.⁶ Compared to the solar cells with local doped regions formed by photolithography and diffusion, however, laser processed solar cells usually exhibit a lower efficiency, which can be attributed to the increased bulk recombination at the laser doped regions caused by the laser-induced defects.^{7,8} Our recent simulation results have indicated that the recombination current density of laser doped regions without passivation may be higher than 5000 fA/cm² (even reaching a few tens of thousand fA/cm² with non-optimized laser parameters),⁹ which is

much higher than that of conventional thermally diffused regions. As such, the high recombination at laser doped regions becomes the dominant loss that limits the efficiency of the laser-processed solar cells.

A possible approach to improve the laser-processed solar cells efficiency is to passivate the laser doped regions with an ultra-thin dielectric, which have to be sufficiently thin to allow current flow via quantum mechanical tunnelling whilst being thick enough to provide reasonable surface passivation. At the same time, the laser doping fraction could be enlarged to reduce the effect of the contact resistivity. Up till now, SiO₂, Al₂O₃, and a-Si:H dielectrics have been investigated as passivation layers for boron- or phosphorus-diffused p⁺ and n⁺ regions.¹⁰⁻¹⁴ The results indicated that SiO₂, Al₂O₃, and amorphous silicon (a-Si:H) ultrathin layers with optimized thickness (typically <2 nm) could provide appreciable passivation to diffused p⁺ and n⁺ regions whilst maintaining a relatively low contact resistivity. However, the passivation stability of these ultrathin dielectrics during the final metal contact annealing is still a problem to be resolved before being applied on solar cell fabrication. In this work, the implementation of the passivated contact concept into n-type silicon solar cells with laser-processed LBSF is presented. The recent developed SiO₂/a-Si:H stacks, which have shown excellent passivation to n⁺ regions and good thermal stability,^{15,16} are applied at the laser processed rear side to reduce carrier recombination.

The line-structured n⁺ LBSF was achieved by laser chemical processing (LCP) with diluted H₃PO₄ solution (50%),¹⁷ which could open the dielectric layers and form the LBSF in a single step. The sheet resistance (*R*_s) and contact resistivity (*ρ*_c) of LCP-LBSF with or without SiO₂/a-Si:H stacks were determined by the transfer length method (TLM). The optimal LCP parameters were selected at a scanning speed of 100 mm/s and a laser energy of 23 μJ, by which an *R*_s and *ρ*_c value of 34 Ω/□ and 1.8 × 10⁻⁵ Ω·cm² can be achieved, respectively.¹⁸ To fabricate the TLM structures, p-type wafers (>100 Ω cm) coated with plasma enhanced chemical vapour deposition (PECVD) SiN_x (70 nm) on both sides were patterned with parallel LCP doped lines on one side of the samples. The samples were

^{a)} Author to whom correspondence should be addressed. Electronic mail: xinbo.yang@anu.edu.au Tel.: +61 02 6197 0112. Fax: +61 02 61250506.

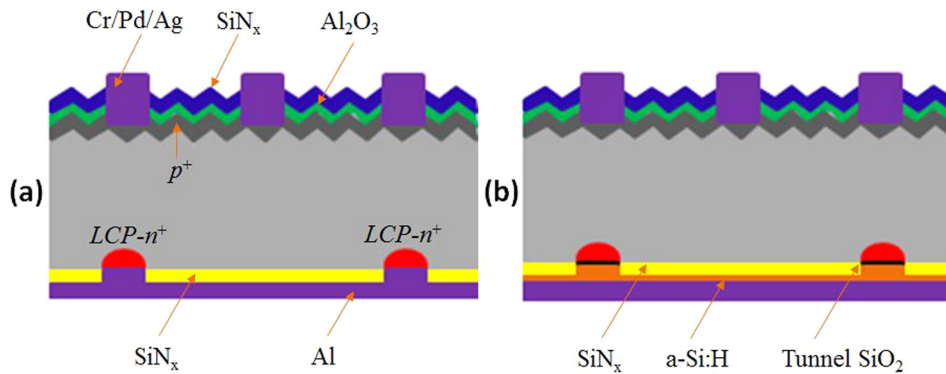


FIG. 1. The structure of the n-type PERL solar cell (a) without and (b) with a passivated contact to the laser-LBSF.

then separated into two groups. One group was coated with the $\text{SiO}_2/\text{a-Si:H}$ stack on the laser-processed side, which was formed by a short thermal oxidation in a clean quartz tube furnace at 800°C for 20 s (~ 1.5 nm) and then capped with a PECVD a-Si:H film (~ 30 nm). TLM patterns were defined for both groups using photolithography after evaporation of aluminium (~ 1 μm) on the laser-processed side. Current-voltage measurements were performed on a Keithley 2425 Source Meter after annealing in forming gas atmosphere (FGA) at different temperatures for different times. The contact resistivity (ρ_c) was obtained from an extrapolation of resistance versus pad spacing.

N-type PERL cells with and without rear passivated contact to laser-LBSF were fabricated on $2.5\ \Omega\cdot\text{cm}$ FZ-Si wafers with a thickness of $\sim 200\ \mu\text{m}$. The cell size is $2 \times 2\ \text{cm}^2$. Figure 1 shows the sketch of n-type PERL solar cells with and without passivated contact to laser-LBSF. The front side was textured with a random pyramid structure and has a boron diffused p^+ emitter with a sheet resistance of $\sim 120\ \Omega/\square$. The p^+ emitter was passivated by an $\text{Al}_2\text{O}_3/\text{SiN}_x$ stack (~ 70 nm), which is formed by atmospheric pressure chemical vapour deposition (APCVD, $\text{Al}_2\text{O}_3 \sim 15$ nm)¹⁹ and PECVD (SiN_x , ~ 55 nm). The front fingers were photolithographically defined and consisted of an evaporated stack of Cr/Pd/Ag further thickened by Ag electro-plating. The rear-side was passivated with PECVD SiN_x (~ 70 nm). Line-structured LBSFs with a pitch of 1.0 and 1.5 mm were applied at the rear-side. A line width of $\sim 45\ \mu\text{m}$ was obtained by LCP. Half of the cells were then subjected to a short thermal oxidation and capped with a-Si:H on the rear-side. Finally, the rear-side of all the cells was metallized with an evaporated aluminum layer ($2\ \mu\text{m}$), and an annealing step at 300°C for 30 min in FGA was performed for contact formation. Light I - V tests were performed under standard AM1.5 illumination using an in-house system. The light source intensity of this system was calibrated using a certified reference cell from Franhauser ISE CalLab.

A crucial parameter in the success of a low ρ_c value for the $\text{SiO}_2/\text{a-Si:H}$ passivated contact is the annealing temperature, which will activate the alloying between a-Si:H and overlying aluminum film to create a high conductivity mixed-phase layer. The lowest temperature at which the a-Si:H/Al alloying, and hence the contact formation will occur, has been shown to be $\geq 250^\circ\text{C}$.¹⁶ A proper annealing temperature must be chosen so that the aluminium interacts with the a-Si:H to achieve a low ρ_c value but not with the underlying thin SiO_2 to maintain a good passivation.

Figure 2 shows the ρ_c dependence on anneal conditions for laser doped n^+ regions with and without $\text{SiO}_2/\text{a-Si:H}$ stack. After annealing at 250°C for 30 min, an acceptable ρ_c value of 5.5×10^{-3} and $1.8 \times 10^{-3}\ \Omega\cdot\text{cm}^2$ could be achieved on the samples with and without the $\text{SiO}_2/\text{a-Si:H}$ stack, respectively. A higher ρ_c value is observed on the sample with the $\text{SiO}_2/\text{a-Si:H}$ stack with the same annealing recipe. As the annealing temperature increases, the ρ_c value decreases continuously in both cases. The low ρ_c values are a result of the high surface concentration ($\sim 4.5 \times 10^{19}\ \text{cm}^{-3}$) of the laser doped regions.¹⁸ We should note that a low ρ_c value of $7.6 \times 10^{-4}\ \Omega\cdot\text{cm}^2$ can be achieved after annealing at 300°C for 30 min, which is the exact annealing recipe we used for contact forming annealing.

With the decreasing ρ_c values after annealing at higher temperatures, it is important to maintain the passivation performance simultaneously. Here, photoluminescence (PL) imaging with a short pass filter (1025 nm) was used to qualitatively monitor the passivation function of annealing conditions after each step, and the passivation quality is determined in terms of the implied open circuit voltage (i - V_{oc}) measured by quasi-steady-state photoconductance (QSSPC) technique. A short pass filter can minimize the effect of rear-side reflection after metallization. Figure 3 shows the PL images of a SiN_x passivated sample after different processing at the rear-side. All the images were acquired with the same PL parameters from the front-side. The processing begins with a quarter silicon wafer

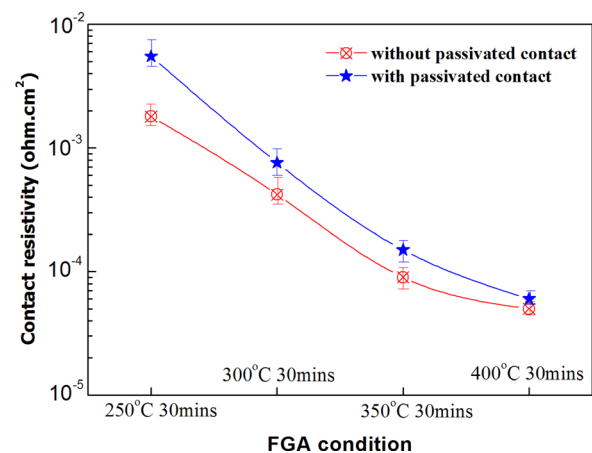


FIG. 2. Contact resistivity dependence on FGA annealing conditions for laser-LBSF with and without $\text{SiO}_2/\text{a-Si:H}$ stack. Lines only provide a guide to eyes.

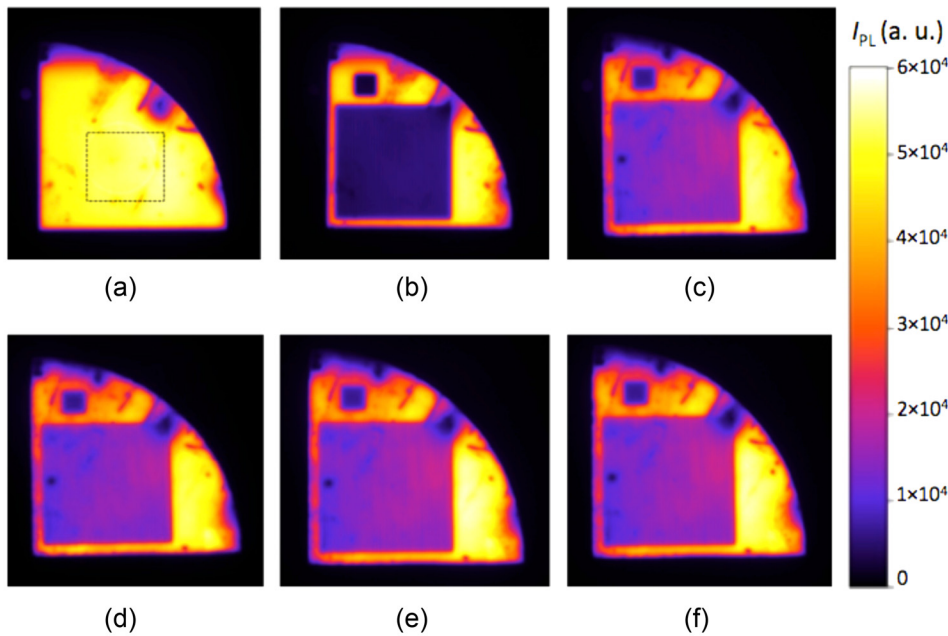


FIG. 3. PL images of SiN_x passivated sample after different processing at the rear-side. All the images were acquired with the same PL parameters. I_{PL} and/or implied open circuit voltage ($i\text{-}V_{\text{oc}}$) values after each step are as follows: (a) SiN_x passivated sample $i\text{-}V_{\text{oc}}$: 708 mV and I_{PL} : 51 000; (b) After LCP, 0.75 mm pitch $i\text{-}V_{\text{oc}}$: 635 mV and I_{PL} : 5000; (c) After $\text{SiO}_2/\text{a-Si:H}$ deposition $i\text{-}V_{\text{oc}}$: 670 mV and I_{PL} : 15 000; (d) After Al metallization I_{PL} : 14 700; (e) After FGA at 250 °C 30 min I_{PL} : 16 000; and (f) After FGA at 300 °C 30 min I_{PL} : 15 600.

(2.5 $\Omega\text{-cm}$) passivated by SiN_x with an $i\text{-}V_{\text{oc}}$ value of 708 mV [Fig. 3(a)]. PL intensity (I_{PL}) and/or $i\text{-}V_{\text{oc}}$ values after each step are shown in the figure. All the I_{PL} values were collected from the area marked by black dashed lines. Parallel LCP doped lines with a pitch of 0.75 mm are applied to form a $30 \times 30 \text{ mm}^2$ area at the rear side [Fig. 3(b)]. A sharp decrease of $i\text{-}V_{\text{oc}}$ (-73 mV) as well as I_{PL} is observed after this step, which can be attributed to the high passivation layer opening fraction ($\sim 6\%$) at the rear as well as the laser-induced defects at the laser doped areas. After the implementation of the $\text{SiO}_2/\text{a-Si:H}$ stack at the rear-side, $i\text{-}V_{\text{oc}}$ value is improved to 670 mV accompanied by an obvious increase in the I_{PL} value [Fig. 3(c)]. The large $i\text{-}V_{\text{oc}}$ gap (38 mV) between the initial sample in Fig. 3(a) and the sample in this step can be mainly attributed to the laser-induced damage, which cannot be recovered by re-passivation. After metallization, $i\text{-}V_{\text{oc}}$ value cannot be measured by QSSPC anymore. The I_{PL} value change can be used to qualitatively monitor the passivation change after metallization and annealing. After rear metallization by aluminium [Fig. 3(d)], only a slight I_{PL} value decrease is observed. The I_{PL} value increases to 16 000 after annealing at 250 °C for 30 min [Fig. 3(e)], which indicates a slight rear passivation improvement. It can also be seen that the alloying between a-Si:H and aluminium at this step does not have any effect on the passivation quality of the $\text{SiO}_2/\text{a-Si:H}$ stack. Further annealing at 300 °C for 30 min leads to a slight I_{PL} value decrease, which indicates that the passivation of the $\text{SiO}_2/\text{a-Si:H}$ stack is stable at this temperature. Therefore, a simultaneous minimization of carrier recombination and contact resistivity to the laser doped n^+ regions could be achieved with the $\text{SiO}_2/\text{a-Si:H}$ stack after annealing at 300 °C for 30 min in FGA.

Although the $\text{SiO}_2/\text{a-Si:H}$ stack allows good contact to laser doped n^+ regions after annealing, the recombination parameters (J_0) at the contact regions still might be higher than 100 fA/cm² due to the laser-induced defects. According to the simulations, a small contact fraction (3%–5%) should be applied to achieve a high efficiency with the

implementation of passivated contacts if J_0 is relatively high and ρ_c is small.^{15,16} Here, we applied the $\text{SiO}_2/\text{a-Si:H}$ passivated contact to n-type solar cells with laser-LBSF at a pitch of 1.5 and 1.0 mm, which corresponds to a contact fraction of 3% and 4.5%, respectively. Table I shows the results of n-type solar cells with and without the passivated contact to laser-LBSF. Without the passivated contact, the cell efficiency is mainly limited by a low V_{oc} , which is caused by the high recombination at the laser doped regions. A relatively low efficiency of 19.7% and 19.4% is achieved with rear contact fraction of 3% and 4.5%, respectively. With the implementation of a passivated contact, the cell V_{oc} , and hence the efficiency are improved significantly. A relatively high efficiency of 20.9% has been achieved with a contact fraction of 4.5%, which means that an absolute efficiency gain of 1.5% has been achieved with the implementation of passivated contact. However, a smaller absolute efficiency gain of 0.6% has been achieved with a smaller contact fraction of 3%. These cell efficiencies are mainly improved due to a V_{oc} increase (up to 44 mV), which is caused by the reduced surface recombination at the laser doped regions by the implementation of the $\text{SiO}_2/\text{a-Si:H}$ passivated contact. Slight J_{sc} improvement is also achieved at the same time. A small loss in FF has been observed for cells with the passivated contacts, which might be attributed to the higher contact resistivity of the $\text{SiO}_2/\text{a-Si:H}$ passivated contact.

In summary, we have implemented the $\text{SiO}_2/\text{a-Si:H}$ passivated contact to n-type solar cells with laser-processed LBSF.

TABLE I. Results of n-type silicon solar cells with and without the $\text{SiO}_2/\text{a-Si:H}$ passivated contact to laser-LBSFs.

Contact fraction	V_{oc} (mv)	J_{sc} (mA/cm ²)	FF (%)	η (%)
3%	641	39.4	78.1	19.7
3% with PC ^a	664	39.6	77.2	20.3
4.5%	630	38.9	79.2	19.4
4.5% with PC	674	39.2	79.1	20.9

^aPC: Passivated contact.

The cells efficiencies have been improved with the implementation of the passivated contact concept, which is mainly attributed to the reduced surface recombination at the laser doped regions. An absolute efficiency gain of up to 1.5% has been achieved with the implementation of the SiO₂/a-Si:H passivated contact. This study demonstrates that the efficiency of solar cells with partial rear contact can be improved with the implementation of the passivated contact concept.

The authors acknowledge financial support from the Australian Renewable Energy Agency (ARENA) under the Postdoctoral Fellowship.

- ¹J. Zhao, A. Wang, and M. A. Green, "24.5% efficiency silicon PERT cells on MCZ substrates and 24.7% efficiency PERL cells on FZ substrates," *Prog. Photovoltaics* **7**, 471–474 (1999).
- ²M. Kim, D. Kim, D. Kim, and Y. Kang, "Influence of laser damage on the performance of selective emitter solar cell fabricated using laser doping process," *Sol. Energy Mater. Sol. Cells* **132**, 215–220 (2015).
- ³D. Lin, M. Abbott, P. H. Lu, B. Xiao, B. Hallam, B. Tjahjono, and S. Wenham, "Incorporation of deep laser doping to form the rear localized back surface field in high efficiency solar cells," *Sol. Energy Mater. Sol. Cells* **130**, 83–90 (2014).
- ⁴G. Xu, B. Hallam, Z. Hameiri, C. Chan, Y. Yao, C. Chong, and S. Wenham, "Over 700 mV implied V_{oc} on *p*-type CZ silicon solar cells with double-sided laser doping," *Energy Procedia* **33**, 33–40 (2013).
- ⁵T. C. Roder, S. J. Eisele, P. Grabitz, C. Wagner, G. Kulushich, J. R. Kohler, and J. H. Werner, "Add-on laser tailored selective emitter solar cells," *Prog. Photovoltaics* **18**, 505–510 (2010).
- ⁶J. Benick, B. Steinhauser, R. Müller, J. Bartsch, M. Kamp, A. Mondon, A. Richter, M. Hermle, and S. Glunz, "High efficiency n-type PERT and PERL solar cells," in *Proceedings of the 40th IEEE Photovoltaic Specialist Conference* (2014), pp. 3637–3640.
- ⁷M. Ametowobla, G. Bilger, J. R. Kohler, and J. H. Werner, "Laser induced lifetime degradation in p-type crystalline silicon," *J. Appl. Phys.* **111**, 114515 (2012).
- ⁸Z. Hameiri, L. Mai, T. Puzzer, and S. R. Wenham, "Influence of laser power on the properties of laser doped solar cells," *Sol. Energy Mater. Sol. Cells* **95**, 1085–1094 (2011).
- ⁹A. Fell, D. Walter, X. Yang, S. Surve, E. Franklin, K. Weber, and D. MacDonald, "Quantitative surface recombination imaging of single side processed silicon wafers obtained by photoluminescence modelling," *Energy Procedia* **55**, 63–70 (2014).
- ¹⁰J. Bullock, D. Yan, and A. Cuevas, "Passivation of aluminium-n⁺ silicon contacts for solar cells by ultrathin Al₂O₃ and SiO₂ dielectric layers," *Phys. Status Solidi RRL* **7**, 946–949 (2013).
- ¹¹F. Feldmann, M. Simon, M. Bivour, C. Reichel, M. Hermle, and S. W. Glunz, "Carrier-selective contacts for Si solar cells," *Appl. Phys. Lett.* **104**, 181105 (2014).
- ¹²D. Garcia-Alonso, S. Smit, S. Bordihn, and W. Kessels, "Silicon passivation and tunneling contact formation by atomic layer deposited Al₂O₃/ZnO stacks," *Semicond. Sci. Technol.* **28**, 082002 (2013).
- ¹³J. Bullock, D. Yan, Y. Wan, A. Cuevas, B. Demareux, A. Hessler-Wyser, and S. De Wolf, "Amorphous silicon passivated contacts for diffused junction silicon solar cells," *J. Appl. Phys.* **115**, 163703 (2014).
- ¹⁴X. Loozen, J. Larsen, F. Dross, M. Aleman, T. Bearda, B. O'Sullivan, I. Gordona, and J. Poortmans, "Passivation of a metal contact with a tunneling layer," *Energy Procedia* **21**, 75–83 (2012).
- ¹⁵J. Bullock, A. Cuevas, D. Yan, B. Demareux, A. Hessler-Wyser, and S. De Wolf, "Passivated contacts to n⁺ and p⁺ silicon based on amorphous silicon and thin dielectrics," in *Proceedings of the 40th IEEE Photovoltaic Specialist Conference* (2014), pp. 3442–3447.
- ¹⁶J. Bullock, D. Yan, A. Cuevas, B. Demareux, A. Hessler-Wyser, and S. De Wolf, "Amorphous silicon enhanced metal-insulator-semiconductor contacts for silicon solar cells," *J. Appl. Phys.* **116**, 163706 (2014).
- ¹⁷D. Kray, A. Fell, S. Hopman, K. Mayer, G. Willeke, and S. Glunz, "Laser Chemical Processing (LCP)-A versatile tool for microstructuring applications," *Appl. Phys. A* **93**, 99–103 (2008).
- ¹⁸X. Yang, A. Fell, E. Franklin, L. Xu, D. Macdonald, and K. Weber, "High efficiency n-type silicon solar cells with local back surface fields formed by laser chemical processing," in *42nd IEEE Photovoltaics Specialist Conference*, New Orleans, 2015.
- ¹⁹L. E. Black and K. R. McIntosh, "Surface passivation of c-Si by atmospheric pressure chemical vapor deposition of Al₂O₃," *Appl. Phys. Lett.* **100**, 202107 (2012).